Polymer Segment Density Distributions in Saturated Polystyrene Latex Systems[1]

Preston Keusch, Robert A. Graff, and David J. Williams*

Department of Chemical Engineering, The City College of The City University of New York, New York, New York 10031. *Received October 24, 1973*

ABSTRACT: It has long been assumed *a priori* that in polystyrene latex systems monomer and polymer mix completely and uniformly, whereas we have compiled evidence to the contrary. For example, seeded emulsion polymerizations, beginning with the second stage monomer charge in equilibrium saturation with seed, generate particles with a core-shell structure in which the second generation polymer overcoats the first. To explain our observations we have suggested that monomer actually encapsulates the seed polymer under equilibrium saturation conditions rather than swelling it uniformly. In this paper we explore the molecular-thermodynamic factors which govern particle morphology. The primary forces appear to originate with the restrictions which the polymer molecules experience in the confined habit of the latex particle as they attempt to occupy their favored random-coil conformations. These forces are described by a surface-dependent free energy of restricted volume term and then compared to the volume-dependent free energy of mixing. Model thermodynamic calculations account for a simple encapsulation model comprised of a core with polymer and limited monomer uniformly mixed surrounded by the remaining monomer in a shell. The level and influence of polymer segment adsorption at the particle-water interface is probably negligible. We consider the form of the overall polymer segment density distribution; both experimental and theoretical analysis indicates that this distribution should be high in the central region of the particle and drop to near zero at the particle-water interface.

As is well known, styrene and polystyrene are fully compatible and ordinarily form homogeneous solutions. Furthermore, if the styrene monomer in such a homogeneous solution were polymerized, both the initially present and the newly formed polystyrene would be uniformly mixed within the other in the final product. We have discovered a system which constitutes an exception to the foregoing generally accepted pattern of behavior, namely, styrene–polystyrene latexes.

The earliest clue of any unusual behavior stemmed from our kinetic studies of styrene emulsion polymerizations.[2a] In the past, it had been generally accepted that styrene and polystyrene are uniformly mixed in a polymerizing latex particle; but, in order to reconcile our results we proposed that a growing latex particle is actually a heterogeneous entity whose morphology could be approximated by a core–shell model. In this model a monomer-rich shell surrounds a polymer-rich core and the monomer-rich shell serves as the major locus of polymerization.

In order to gain further support for the core–shell model and to elucidate the factors controlling particle morphology, we next undertook[2b] a series of seeded styrene emulsion polymerizations in which polystyrene latexes (polymer I) were saturated with fresh styrene (monomer II) and equilibrium was attained before the second-stage polymerization (converting monomer II to polymer II) was initiated. Potassium persulfate was the usual initiator, and the weight fraction monomer in the second-stage charge was about 0.73. Two methods were employed to distinguish between the first- and second-generation polystyrene: butadiene tagging coupled with ultramicrotomy and osmium tetroxide staining plus tritiated styrene tagging coupled with autoradiographic detection techniques. To reiterate, for emphasis, the important features of these seeded polymerizations are that polymers I and II as well as monomer II are fully compatible and ample time (48 hr) was allowed for the attainment of equilibrium saturation before polymerization was reinitiated. Contrary to what one might have expected, polymers I and II were not uniformly mixed in the final latex particles, but polymer II overcoated polymer I in a core–shell fashion. Furthermore, the core diameters corresponded to the original seed diameters, and there was no evidence of appreciable polymer I–polymer II interpenetration between the core and shell; hence, the major portion of polymer II located within the shell. These morphological features were found to persist over a wide range of conditons: namely, viscosity-average molecular weights from 20,000 to 10^7, particle diameters from *ca.* 500 to 6500 Å, and butadiene level in the monomer II charge from 0.7 to 50 wt %.[3]

The fact that a definite particle morphology persists even when the second-stage polymerizations emanated from a condition of equilibrium saturation suggests that particle morphology is controlled by molecular thermodynamic factors and not by a diffusion-controlled kinetic mechanism.[2b] Theoretical arguments have been presented that also discount the possibility of control by a kinetic mechanism.[4,5]

In order to explain the core–shell morphology we postulated that at equilibrium saturation before the second stage polymerization is initiated, monomer II overcoats or encapsulates polymer I rather than swelling it uniformly. By way of an alternate explanation we also considered the possibility that polymer I and monomer II are uniformly mixed at saturation and that it is the growth mechanism which leads to the core–shell structure.

In this paper attention focuses primarily on the seeded styrene emulsion polymerizations.[2b] We accept as definitive the experimental evidence that the second-generation polymer overcoats the first-generation polymer in the final latex. It remains to establish the mechanism by which this overcoating process occurs. Here we review and clarify the arguments for the two possible mechanisms already suggested and present additional thermodynamic arguments supporting the encapsulation model. Another mechanism might be operating which has not been suggested. No definitive theoretical explanation or experimental evidence is yet available to decide between the two possibilities; but at this time the weight of the evidence appears to favor the encapsulation model.

One of the difficulties and sources of uncertainty faced in this work is that we are attempting to infer a morphology for the saturated latex particle from studies of the final latex product. Although, the detailed morphology of the saturated state remains obscured because of this limitation certain elements of the gross morphological features readily emerge, and these are the features we wish to discuss.

Another bit of factual information is germane to the ensuing discussion. Recall from the studies of van den Hul

and Vanderhoff[6] plus Ottewill[7] that with persulfate initiation the major portion of sulfate end groups remains on the surface of the particles—even through successive generations of seeded polymerizations. This means that nearly all the polymer molecules are bound to the particle water interface by their chain ends.

I. Proposed Mechanisms for the Overcoating Process

A. Growth-Oriented Mechanism. As a possible explanation one could postulate that monomer and polymer are uniformly distributed at equilibrium. Upon reinitiation, growth of a polymer chain begins at the surface as an oligomeric sulfate radical enters the particle. Continued growth occurs in the vicinity of the interface because the polymer chains are anchored to the particle surface. As monomer II in the vicinity of the interface is consumed, monomer II in the central region diffuses toward the polymerization site, displacing polymer I chains toward the central region of the particle. Hence, as polymerization progresses, polymer II chains grow and remain in the peripheral region by virtue of their attachment to the surface while polymer I chains collect in the center.

This explanation encounters serious difficulties because polymer I and polymer II chains are identical. They are both attached to the surface and they both assume random-flight conformations (subject to the physical constraints imposed by the crowded and confined habit of the latex particle). A chain segment associated with a growing polymer II chain is not imbued with any properties to distinguish it from chain segments associated with polymer I chains or inactive polymer II chains. The incorporation of tritiated styrene as a tagging agent does not impart a distinction with respect to driving forces for diffusion or phase separation. We have argued elsewhere[2b,5] that the use of butadiene does not impart distinguishing properties with respect to either diffusion or phase separation. Hence, there are no property differences between polymer I or polymer II chains that can serve as a driving force for diffusion or spontaneous phase separation. This implies that if growth of a polymer II chain caused a depletion of monomer II in the vicinity of the particle surface and diffusion from the central region to the particle surface, both polymer I and polymer II chain segments should be displaced toward the center without discrimination. Hence, a well mixed initial particle environment should not lead to the sharply defined core–shell regions observed in the final particle.

Another matter to discuss is the relative mobility of the various reacting species. If polymer diffusion did occur, it would have to operate against the built-up concentration gradients as the selective migration proceeded, and this diffusion would have to occur in a very viscous environment which would become increasingly viscous and eventually glass like as the polymerization progressed to completion.

B. The Encapsulation Model. Alternatively, one could postulate that monomer II does not uniformly swell the particle but the major portion of monomer II is located in the peripheral region at saturation. Upon reinitiation monomer II converts to polymer II in the peripheral region, thus forming a core–shell structure. This model is similar to the growth oriented mechanism just discussed in that both require the second stage polymerization to occur in the vicinity of the particle surface. The encapsulation model requires the establishment of polymer I–monomer II gradients prior to repolymerization whereas the growth-oriented model requires the establishment of polymer I–polymer II gradients during the second stage of polymerization. We have just argued against the latter, and we devote the remainder of this paper to describing how monomer–polymer gradients might form upon saturation.

Before proceeding, we review briefly the experimental evidence favoring an encapsulation model. (a) The notion of a monomer-rich interfacial region, perhaps a few hundred ångstroms thick, is in accord with core–shell model which we postulated on the basis of kinetic evidence.[2a] (b) The growth-oriented model is based on the fact that initiation occurs at the particle–water interface; and, since the chain is permanently bound there, it continues to grow in a region close to the interface. In the encapsulation model initiation at the interface and attachment of the polymer chain to the interface are of secondary importance. Of primary importance is the initial distribution of monomer II and polymer I. To distinguish between these two explanations we performed a seeded polymerization experiment in which an oil-soluble initiator (benzoyl peroxide) was used to initiate the second stage of growth. The prevalence of the core–shell morphology in the final latex again favors the encapsulation model.[2b]

II. Thermodynamic Considerations

As previously stated, the fact that a definite particle morphology persists even when the second stage of polymerization emanates from equilibrium saturation conditions strongly suggests that particle morphology is controlled by molecular thermodynamic factors. The remainder of this paper is devoted to exploring this view point.

Of overriding importance is the fact that we are dealing with a microscopic thermodynamic system and not one of macroscopic proportions. In such a system, forces operating at or near the interface can outweigh those which operate within the volume of the system. For a given level of particle saturation, we assume that the surface free energy remains constant. Two opposing forces are in operation. The volume-dependent free energy of mixing causes mixing and conformational constraints cause demixing. We have previously introduced the latter as "entropic considerations."[2b] The demixing force is surface area dependent, and it originates in the long-chain conformational properties of the polystyrene molecules and their interactions with the particle interface.

Note that two kinds of polymer segment density distributions must be considered: one describes the overall distribution within the particle for all the molecules and the second describes the conformations of the individual molecules. Of paramount importance in establishing the overall polymer segment density distribution is the desire of the individual polymer molecules to occupy random-coil conformations. In the case of the saturated latex particle the ability of the individual chains to occupy their prefered conformations is hindered by the confined and crowded habit of the latex particle and by the fact that all chains are attached to the interface. We shall discuss this problem later in this paper. Recognize at the outset that in order to achieve a *uniform* overall segment density distribution, the density distribution for that portion of molecules near the interface must be unnaturally compressed. Only those molecules located near the center—sufficiently distant from the interface—can have a Gaussian segment density distribution.

A distribution model more entropically favored would consist of a dense central network of entangled, coiled polymer chains surrounded by a peripheral shell consisting of a dilute network of polymer chains whose centers of mass were sufficiently far removed from the interface so as to allow them to occupy their prefered random-coil conformations.

The general problem of describing restricted-chain con-

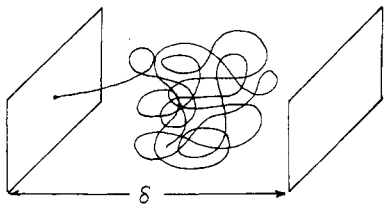

Figure 1. A random polymer chain between two impenetrable, parallel plates, separated by a variable plate distance δ, attached by one chain end to the left-hand plate.

formations within a thermodynamic framework suitable to the present situation has been provided by Meier.[8] His work provides a means of quantitatively comparing the free energy of mixing to the free energy resulting from what we have referred to as "entropic considerations."[2b]

Meier has calculated the *free energy of restricted volume*, $\Delta G_v(\delta)$ of a polymer molecule between two parallel plates separated by a distance, δ, compared to the free energy if the plates were infinitely separated (Figure 1). The plates are impenetrable and their surfaces are noninteracting with respect to the polymer. In this analysis the molecule is attached to one plate at one chain end. For a flexible long-chain molecule, such as polystyrene, random-flight statistics are applicable. The required chain statistics are generated by the diffusion equation

$$\partial W(\bar{r})/\partial N = (l^2/6)\nabla^2 W(\bar{r}) \tag{1}$$

for $W(\bar{r})$ the probability of the end-to-end distance being $\bar{r}$, for N segments of length l.

As the surface containing the attached chain is brought closer to the other surface, the volume available to the chain decreases; and as a result, certain chain conformations will be excluded. At a separation distance, δ, the fraction of allowable chain conformations will just be equal to the probability $P_N(\delta)$ that all elements of the attached chain are within a distance δ of the surface compared to when the other surface is at infinity. This probability can be determined from the diffusion equation as follows. First obtain the conditional probability $W_N(x,r;x',0;\delta)dV$ of finding the free end of the chain of N segments in the volume element dV at x,r in cylindrical coordinates when the first end is at $x = x'$ and $r = 0$. The boundary conditions for this problem are

$$W_N(0,r;x',0;\delta) = W_N(\delta,r;x',0;\delta) = 0 \tag{2}$$

These conditions also exclude from the ensemble those conformations for which any of the segments has reached the boundaries at $x = 0$ or δ.

The solution to eq 1 and 2 is normalized for $\delta = \infty$. Since we want the first chain end to be at $x = 0$ we let $x' \rightarrow 0$. With the solution for $W_N(x,r;0,0;\delta)dV$, we find $P_N(\delta)$ as follows

$$P_N(\delta) = 2\pi\int_{r=0}^{\infty}\int_{x=0}^{\infty} W_N(x,r;0,0;\delta)r\,dr\,dx \tag{3}$$

From the Boltzman relation

$$\Delta G_v(\delta) = -T\Delta S_v(\delta) = -kT\ \ln\ (P_N(\delta)) \tag{4}$$

where $\Delta S_v(\delta)$ corresponds to our "entropic considerations." The result obtained is as follows

$$\frac{\Delta G_v(\delta)}{kt} = -\ln \sum_{m=-\infty}^{m=+\infty}\left\{\exp\left[\frac{-6m^2\delta^2}{Nl^2}\right] - \exp\left[\frac{-3(2m-1)^2\delta^2}{2Nl^2}\right]\right\} \tag{5}$$

which is shown graphically in Figure 2. From this result it is seen that if a long-chain molecule is confined in too

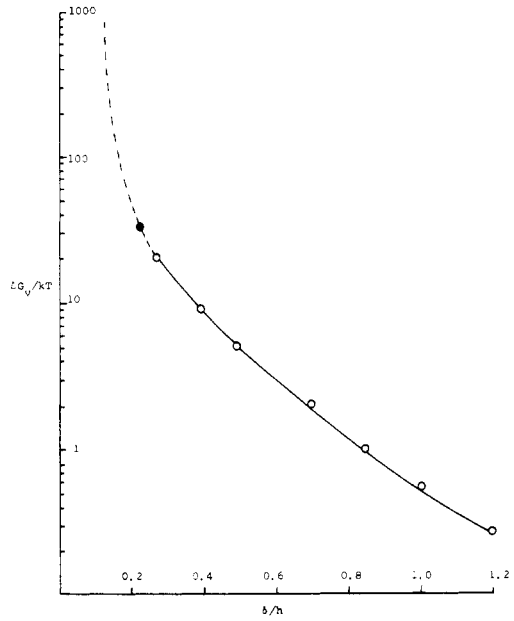

Figure 2. Free energy of restricted volume *vs.* distance of plate separation per mean-square end-to-end distance.

small a space, *i.e.*, $\delta \rightarrow 0$, a large positive free energy would result rendering that situation thermodynamically unlikely.

Considerable difficulty is encountered in obtaining a numerical solution for eq 5 for $\delta/h < 0.27$. The solid line in Figure 2 is Meier's solution. We have duplicated his solution and extended it to $\delta/h = 0.218$ with $\Delta G_v/kT = 32.15$, shown as the solid point. The dashed line is the extrapolation used in our model calculations. We are currently attempting to extend the calculations to lower values of δ/h.

The analogy between the situation Meier described and the situation under consideration is depicted in Figure 3. Instead of a variable plate separation, we have a variable shell thickness. With $\delta = 0$ mixing is complete and a uniform segment density distribution is obtained. The maximum value of δ is obtained with pure polymer core and a pure monomer shell. With intermediate values of δ, we will assume as a first approximation that uniform mixing of monomer and polymer occurs in the core and only monomer is found in the shell. As we will consider later, some intermixing does apparently occur and the sharp interface required to define δ in the context of Meier's analysis does not in reality exist. Likewise the internal core-shell interface (corresponding to the right-hand plate in Figure 1) is not in reality impenetrable. All these approximations are required, however, in the ensuing calculations.

The accepted concept for latex-monomer swelling is that equilibrium is reached when the change in free energy of mixing and the change in surface free-energy balance.[9,10] Analytically this concept is expressed as

$$\Delta G_s = \Delta G_m V + \Delta G_\gamma s \tag{6}$$

where ΔG_s is the free energy of saturation, ΔG_m is the free energy of mixing, ΔG_γ is the change in surface free energy, s is the surface area, and V is the particle volume. At saturation $d\Delta G_s = 0$ and $\Delta G_m dV = -\Delta G_\gamma ds$ as stated. The Flory-Huggins equation is employed to represent ΔG_m. Considering the difficulties involved in obtaining independent estimates of the parameters and the weakness of the Flory-Huggins theory, reasonably good experimental corroboration has indeed been obtained for eq 6.

Table I
System Free Energy $\Delta G_F/RT$ Comparing Free Energy of Restricted Volume to That of Mixing *vs.* Reduced Shell Thickness at [M] = 0.40 and 0.73

				[M] = 0.40		[M] = 0.73	
δ (Å)	δ/h	$\Delta G_v/kT$	$\Delta G_v/RT$ $\times 10^{-16}$	$-\Delta G_m'/RT$ $\times 10^{-16}$	$\Delta G_F/RT^a$ $\times 10^{-16}$	$-\Delta G_M'/RT$ $\times 10^{-16}$	$\Delta G_F/RT^a$ $\times 10^{-16}$
10	0.026	$>10^5$	>5.28	0.1674	>5.115	0.2074	>5.073
30	0.079	10^5	5.28	0.1604	5.120	0.2066	5.073
50	0.131	500	0.0264	0.1543	−0.127	0.2045	−0.178
70	0.183	70	0.0037	0.1471	−0.143	0.2046	−0.201
90	0.236	32	0.0017	0.1390	−0.137	0.2042	−0.203
100	0.262	22	0.0012	0.1343	−0.133	0.2029	−0.202
120	0.314	14.5	0.0008	0.1237	−0.123	0.2017	−0.201
140	0.366	10	0.0005	0.1108	−0.110	0.2016	−0.201
150	0.393	8.6	0.0005	0.1034	−0.103	0.2003	−0.200
200	0.524	4.2	0.0002	0.0466	−0.0462	0.1962	−0.200

[a] $\Delta G_F/RT = \Delta G_v/RT + \Delta G_m'/RT$.

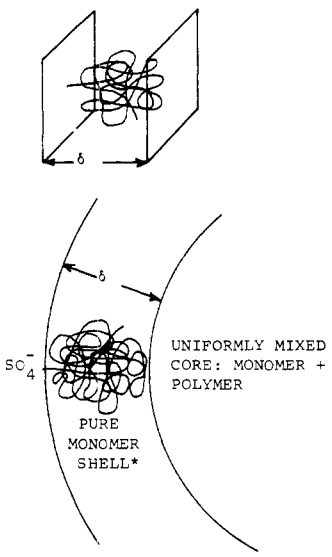

Figure 3. Encapsulated latex particle used in model calculations. *Free energy of mixing for the shell volume is neglected in the calculations.

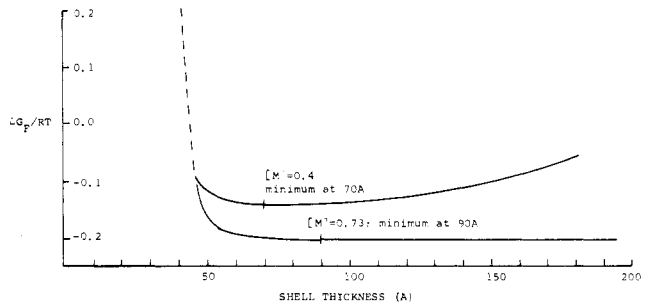

Figure 4. Free-energy curves showing a minimum for $\delta \neq 0$ for two monomer concentrations.

This is not to say, however, that it completely represents the situation.

We suggest generalizing eq 6 by including Meier's term for the free energy of restricted volume $\Delta G_v(\delta)$ which the polymer chains experience near the interface, where δ refers to the shell thickness. Equation 6 then becomes

$$\Delta G_s = \Delta G_m V + \Delta G_\gamma s + \Delta G_v(\delta)s \qquad (7)$$

As shown in Figures 2 and 3 if uniform mixing occurs $\delta \rightarrow 0$, $\Delta G_v/kT$ rises steeply, approaching infinity, and the ΔG_v term in eq 7 dominates the others. Since ΔG_v is positive, ΔG_s would likewise become positive and mixing would be unlikely. On the other hand, as δ approached its maximum value $\Delta G_v/kT \rightarrow 0$, and eq 7 would reduce to eq 6. The latter rationale is in accord with the fact that eq 6 is a reasonable approximation under equilibrium saturation conditions. Model calculations described in the next paragraph support this assertion.

We have considered the free energy of demixing a model latex particle from a homogeneous system to one with a core comprised of monomer and polymer uniformly mixed and a shell comprised of only monomer. The free-energy change of such a transformation $\Delta G_F/RT$ is given by

$$\Delta G_F/RT = (\Delta G_m'/RT) + n(\Delta G_v/kT) \qquad (8)$$

where $\Delta G_m'$ is the free-energy change due to demixing that occurs when a shell of thickness δ forms and n is the number of polymer molecules attached to the particle surface. Presented in Table I and Figure 4 are the results of calculations for two levels of monomer swelling. See the Appendix for details. Observe that a minimum in free energy occurs at shell thickness values of 70 Å and 90 Å for the 0.40 and 0.73 values of weight fraction monomer, respectively. These equilibrium values of shell thickness place about 19.3% of the total monomer in the shell for the 0.40 case and about 35.6% for the 0.73 case. Note from Table I that at equilibrium the ΔG_v term is small compared to $\Delta G_m'$ in accord with our preceding rationale. In general $\Delta G_v(\delta)$ can be neglected in two circumstances: in macroscopic systems where $s/V \rightarrow 0$ and when $\delta \gg h$, where h is the root-mean-square end-to-end distance. The latter arises when δ is large or when molecular weight becomes sufficiently low.

The foregoing calculations should not be construed as proof of the encapsulation phenomenon. We have simply concocted a model thermodynamic system that predicts phase separation because of the importance of restricted volume effects. Nonetheless we believe the model renders valuable insights into the factors governing latex particle morphology.

III. Segment Distributions near an Interface with Segment Adsorption

An assumption used in the last section was the absence of any adsorption interactions. Such interactions would cause the segment distribution to skew away from the core toward the interface. In this section we consider in a general way the segment distributions for a polymer chain located near an impenetrable flat interface, allowing for segment adsorption at the surface. DiMarzio and McCrackin[11] have determined the segment density distributions for long-chain flexible molecules, which have one

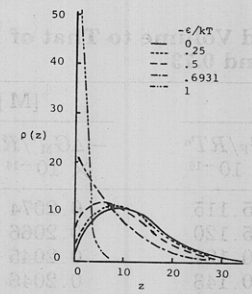

Figure 5. Distribution of density $\rho(z)$ of polymer segments *vs.* distance z from the surface for various values of adsorption energy for chains of 200 segments. For adsorption energies less than the critical value of kT ln 2, the curves have similar shapes and pass through a maximum. For adsorption energies greater than 0.693 kT, most segments lie close to the surface.

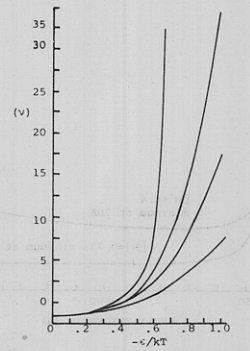

Figure 6. Average number (ν) of contacts with the surface *vs.* the energy of adsorption in units of kT for chains of 50, 100, and 200 segments. The theoretical curve for infinite chain lengths (∞) is also shown.

chain end fixed to a surface, as a function of distance, molecular weight, and attractive energy of the surface. Monte Carlo methods were used in the execution of their model calculations.[12] Figure 5 displays the polymer segment density as a function of distance from the surface for various values of attractive energy; Figure 6 shows the average number of segment contacts at the surface as a function of attractive energy with chain length as a parameter. The pertinent feature of their results is that for energy values of $-\epsilon/kT < ca.$ 0.6 the polymer segment density $\rho(z)$ approaches zero and the number of adsorption contacts approaches one at the surface of attachment.

The low values for adsorption contacts and segment density for values of $-\epsilon < ca.$ 0.6 kT indicates that there is very little polymer near the surface even for systems where the interaction energy is the same magnitude as the energy associated with van der Waal's type forces.

The result for $\epsilon = 0$ is particularly interesting in that the mean square end-to-end distance, $\bar{R}^2$, can be calculated directly. The resulting mean-square end-to-end distance is twice that of the same polymer in the absence of an interface. Thus, the wall forbids all conformations from crossing it, thereby giving preference to conformations on just one side. Since many conformations that would have crossed the wall are forbidden, there will be a low segment density near the wall and the maximum segment density will shift away from the wall.

The experimental evidence produced for the styrene–polystyrene latex system under study shows that there is low concentration of polymer in the peripheral region of the latex. This behavior would be expected for systems with low values of interaction energy ($-\epsilon/kT < 0.6$). Based upon the organochemical structures of the system under investigation, we would expect the interaction to be minimal. We cannot conceive of the polystyrene segments

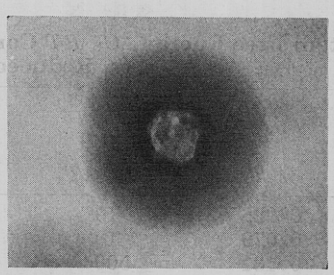

Figure 7. Ultra-thin cross-section of a latex particle containing 10 wt % butadiene in the monomer II charge. The core–shell morphology is clearly discernible. Secondary morphological features—core inclusions and ring around the core—arise from polymer I–polymer II incompatibility and are evidence that the core does contain some monomer II at saturation.

participating in any kind of hydrogen bonding or chemadsorption with the hydrophilic interface or its surfactants. In fact, polystyrene, like most hydrophobic polymers, would be expected to be repelled by water as evidenced by its high contact angle with water. Thus, for the system of interest the adsorption energy of polymer segments with the surface is probably low.

IV. Overall Segment Density Distribution

We now consider the experimental evidence and theoretical arguments which bear on a description of the overall segment density distribution. Several elements of the experimental evidence could have been reconciled by a model consisting of a solid polymer core surrounded by a pure monomer shell: *e.g.*, the kinetic evidence that prompted the postulation of a core–shell morphology. Such an extremely distributed structure can be rejected on at least two counts. Van den Hul and Vanderhoff[6] plus Ottewill[7] have shown for persulfate-initiated styrene emulsion polymerization that nearly all of the polymer chain ends are located on the surface. If the bulk of the polymer is located in the core and the polymer chain ends locate on the surface, then polymer chain segments must permeate the intervening monomer layer.

A pure polymer core can be excluded as well. Saturation seeding experiments of the sort described here with sufficient butadiene—*ca.* 10%—to introduce polymer–polymer incompatibility[13] and oil-soluble initiator runs[2b] form the bases for this assertion. With reference to incompatibility effects[13] Figure 7 shows an ultra-thin cross-section obtained for seeded polymerizations containing 10% butadiene in the monomer II charge. The core–shell structure is clearly evident. One can also observe dark gains in the core which are attributable to the polymer–polymer incompatibility introduced during the second stage of polymerization. That is, some of the 90:10 styrene–butadiene comonomer II mix must have located in the core region during saturation and polymerized largely *in situ* to produce a copolymer incompatible with the polystyrene of the first generation core.

As for the oil-soluble run, the shell obtained after polymerization was smaller than would have been expected with a pure polymer I core indicating that some second-stage polymerization occurred in the core. Hence, some monomer must have located in the core during saturation.

On the basis of the experimental evidence reviewed in this paper we suggest the encapsulation model shown in Figure 8. The model incorporates sulfate end groups on the surface and chain segments that permeate the monomer-rich shell. The individual chains are depicted in their preferred random-coil conformations. Also shown is our qualitative conception of how the overall segment density distribution might look—high in the central region, drop-

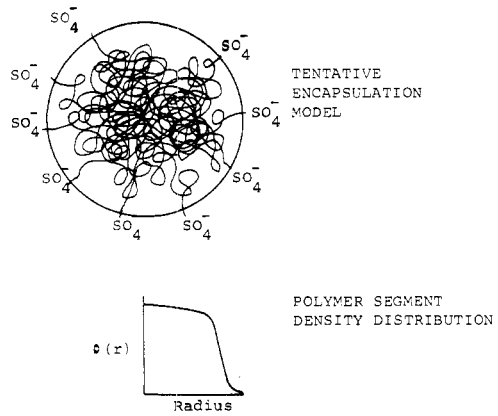

Figure 8. Tentative model for the encapsulation phenomenon. The SO_4^- end groups are located on the particle surface. The individual chains occupy random-coil conformations—subject to the restraints imposed by the microscopic latex particle. The overall segment density distribution is high in the central region, drops off sharply, and approaches zero at the particle surface.

ping off slowly at first and then suddenly to form an interfacial region between the core and shell zones and finally approaching zero at the particle–water interface.

Additional work by Meier on spherical domain formation in block copolymers[14] gives some theoretical insights into the problem. The required assumptions are that end groups are fastened to the surface, that random-flight statistics are applicable and that there is no significant adsorption energy between polymer segments and the surface. The required chain statistics are generated by the diffusion equation for $W(N,\bar{r},\bar{r}',R)$, the probability of finding the free end of a chain of N segments at $\bar{r}$ with the fixed end at $\bar{r}'$. R is the particle radius. The appropriate boundary condition for chains confined to the interior is

$$W(N,R,\bar{r}',R)=0 \tag{9}$$

which also excludes from the ensemble those conformations for which any segment has reached the boundary at R. The segment density, ρ of a single chain of σ_A segments is obtained by summing W over N

$$\rho(\sigma_A;\bar{r},\bar{r}',R)=\sum_{N=1}^{\sigma_A} W(N;\bar{r},\bar{r}',R) \tag{10}$$

The total (overall particle) segment density $\Omega(\sigma_A;\bar{r},R)$ is the sum of the number densities ρ contributed by each chain in the particle with the chain origin $\bar{r}'$ fixed at the surface. Overlap of adjacent molecules causes the angular dependence of segment density to become negligible for more that 24 chains whose origins are equidistant from each other on the surface of the sphere. The normalized density is

$$\Omega'=\left(\frac{4\pi R^3}{3\sigma_A N_A}\right)\Omega \tag{11}$$

where N_A, the number of chains, is independent of chain length for $\sigma_A > 20$ and negligibly dependent on placement of the chain end for $r'/r > 0.9$.

Figure 9 (curve a) shows Ω' as a function of radius r/R for $(\sigma_A l^2)^{1/2}/R$, the ratio of the root-mean-square end-to-end chain distance to the particle radius, equal to 0.6 (an intermediate value for the situation under consideration). The region of low density at the center of the particle is a region of very high energy and will not occur. It arises from the use of purely random-flight statistics and would be smoothed out by chain perturbations if the solution potential (free energy of mixing) were included in the calculation (a far more difficult problem). The effect of the wall is lost as one approaches the particle center, allowing unconstrained polymer segment–monomer mixing. This surface free mixing near the center will decrease free energy and smooth out concentration gradients. The solution potential in effect pulls chain segments toward the center. The result is a nearly uniform density of segments over most of the particle which drops sharply to zero at the outer surface. Curve b of Figure 9 shows this distribution qualitatively. Thus, in accord with the experimentally derived model depicted in Figure 8, Meier's analysis shows an overall segment density distribution for the saturated latex particle which is high in the center and drops to zero at the surface.

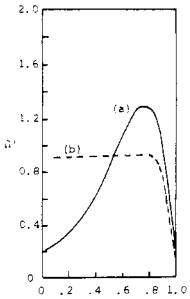

Figure 9. Relative density of segments for $h/R = 0.6$. $(\sigma_A l^2)^{1/2}/R = h/R$.

V. Conclusions

Seeded styrene emulsion polymerizations generate latex particles in which the second-generation polymer overcoats the first in a core–shell fashion. Two possible explanations for this observed morphology were considered: a growth-oriented mechanism and monomer encapsulation of the seed particles at equilibrium saturation. The experimental evidence and theoretical rationale we have presented support the encapsulation model. The primary forces controlling particle morphology are apparently derived from the conformational properties of the polystyrene molecules and their interactions with the particle–water interface. This hypothesis was used to devise a model thermodynamic system that accounts for an encapsulated morphology consisting of a core with monomer and polymer uniformly mixed surrounded by a pure monomer shell. We argue that the level and effect of polymer segment adsorption at the particle–water interface is probably negligible and that, accordingly, the individual segment density distributions should be skewed away from the interface as the polymer molecules attempt to occupy their preferred random-coil conformations. Various elements of the overall segment density distribution were considered, and a conceptual model for the encapsulated latex particle at equilibrium saturation was presented. An essential feature of this model is an overall polymer segment density distribution which is high in the central region of the particle and falls to near zero at the particle–water interface.

Acknowledgments. This paper is based on Ph.D. thesis of Preston Keusch, The City College of The City University of New York, 1973. The work was supported by the National Science Foundation under Grant GK-17582. We thank Dr. D. J. Meier for the fruitful discussions and his helpful suggestions.

VI. Appendix

Free-Energy Calculations for Styrene–Polystyrene Latex Systems. These model calculations are based on a

particle size and molecular weight characterized by experiment. Particle radius R_∞ = 980 Å, $\bar{M}_v = 2.585 \times 10^6$, and $\bar{M}_n = 0.783 \times 10^6$ (based on $\bar{M}_v/\bar{M}_n = 3.3$).[15] Two (weight fraction) monomer levels were used: 0.73 (saturation) and 0.4.

From a mass of monomer and polymer uniformly mixed at a given weight fraction of monomer [M], remove enough material to form a sphere of radius R. The sphere is to consist of a core of monomer and polymer uniformly mixed and shell of pure monomer. Hence, a free energy of mixing $\Delta G_m'/RT$ will result from this segregation. Since the long-chain molecules are bound to the particle interface and they are confined near a surface, there will be a free energy of restricted volume $\Delta G_v/RT$. Other free energies such as that of surface formation and placement of chain ends on the surface will be constant in this analysis. Essentially, we are concerned with the effect demixing has in reducing volume restriction of the polymer molecules within the spherical domain.

The $\Delta G_m'/RT$ term in eq 8 can be approximated by the Flory–Huggins relation

$$\Delta G_m'/RT = N_1' \ln v_1' + N_2' \ln v_2' + \chi v_1' v_2' \quad \text{(A-1)}$$

where χ = an interaction parameter, N_1' = moles of monomer in core, N_2' = moles of polymer in core, V_1' = volume fraction of monomer in core, v_2' volume fraction of polymer in core. The moles and volume fractions will be expressed in terms of the hypothetical shell thickness, δ, of pure monomer. These will in turn allow us to relate $\Delta G_F/RT$ to δ. χ was assigned a value of 0.42.

The radius R of the swollen latex particle can be found by direct use of the definition of weight fraction of monomer

$$[M] = \frac{\frac{4}{3}\pi(R^3 - R_{oo}^3)\rho_m}{\frac{4}{3}\pi(R^3 - R_{oo}^3)\rho_m + \frac{4}{3}\pi R_{oo}^3\rho_p} \quad \text{(A-2)}$$

where R_{oo} is the radius of the "dry" latex seed. With R known one can then partition the system into a polymer core swollen with monomer to thickness R_o and a pure monomer shell of thickness δ in which $R_o = R - \delta$.

$$N_2' = \frac{\frac{4}{3}\pi R_{oo}^3\rho_p}{M_2} = \text{moles of polymer, all in the core} \quad \text{(A-3)}$$

$$N_1'' = \frac{\frac{4}{3}\pi(R^3 - (R-\delta)^3)\rho_m}{M_1} = \text{moles of monomer in the shell} \quad \text{(A-4)}$$

$$N_1 = \frac{1}{M_1}\frac{N_2'M_2[M]}{1-[M]} = \text{overall moles of monomer in the system} \quad \text{(A-5)}$$

then

$$N_1' = N_1 - N_1'' \quad \text{(A-6)}$$

where M_1 is the molecular weight of monomer and M_2 is the molecular weight of polymer. The volume fractions are given as follows

$$v_1' = \frac{N_1'}{N_1' + xN_2'}$$

and (A-7)

$$v_2' = 1 - v_1'$$

where $x = M_2/M_1$.

To calculate the second term of eq 8, we assumed that n is equal to twice the total number of moles of polymer in the system, since all molecules are attached to the surface at both ends. The energy term $(\Delta G_v/kT)$ is found directly from Figure 2 as a function of (δ/h), where h is the mean end-to-end distance of the polymer. Extrapolation was used for $\delta/n < 0.2$. Recognize that $(\Delta G_v/kT)$ has been determined for planar geometry, but we use it only because this function is not available for spherical systems. This value should be more pronounced in spherical systems as curvature will restrict the polymer conformations in more than one dimension. The value of h is based on one-half the molecular weight of the polymer, since all polymer chains are attached to the interface at both ends. For a polystyrene molecule of $\bar{M}_n = 0.220 \times 10^6$ in a good solvent, R_G, the mean radius of gyration, is 115 Å and h is 328 Å. $(\Delta G_F/RT)$ is tabulated *vs.* δ in Table I and plotted in Figure 4 for values of [M] = 0.40 and 0.73.

VII. References and Notes

(1) Presented in part at the Fifth Northeast Regional Meeting of the American Chemical Society, Rochester, N.Y., Oct 1973.
(2) (a) M. R. Grancio and D. J. Williams, *J. Polym. Sci., Part A-1*, **8**, 2617 (1970). (b) P. Keusch and D. J. Williams, *J. Polym. Sci., Polym. Chem. Ed.*, **11**, 143 (1973).
(3) Preston Keusch, Ph.D. Thesis, The City University of New York, 1973.
(4) J. L. Gardon, *J. Polym. Sci., Polym. Chem. Ed.*, **11**, 241 (1973).
(5) D. J. Williams, *J. Polym. Sci., Polym. Chem. Ed.*, submitted.
(6) J. J. Van den Hul and J. W. Vanderhoff, *Brit. Polym. J.*, **2**, 121 (1970).
(7) R. H. Ottewill, University of Bristol, private communication.
(8) D. J. Meier, *J. Chem. Phys.*, **71**, 1861 (1967).
(9) M. Morton, S. Kaizerman, and W. M. Altier, *J. Colloid Sci.*, **9**, 300 (1954).
(10) J. L. Gardon, *J. Polym. Sci., Part A-1*, **6**, 2859 (1968).
(11) E. A. DiMarzio and F. L. McCrakin, *J. Chem. Phys.*, **43**, 539 (1965).
(12) A maximum of 200 steps were used, which corresponds to the evaluation of a polymer of approximately 20,000 molecular weight. This relatively low number of steps is adequate for our problem, since the conformational properties generated at this number have been found to differ very little from those conformational properties that could be calculated by theory at infinite molecular weight.
(13) P. Keusch, J. Prince, and D. J. Williams, *J. Macromol. Sci. Chem.*, **7**, 623 (1973).
(14) D. J. Meier, *J. Polym. Sci., Part C*, **26**, 81 (1969).
(15) M. R. Grancio and D. J. Williams, *J. Polym. Sci., Part A-1*, **8**, 2733 (1970).